alkyl–mercury bond in the series of $RHgCH_3$ including $MeHgCH_3$ $EtHgCH_3$ i-$PrHgCH_3$ t-$BuHgCH_3$ varies 1.0:3.5:2.2:0.1 in a nonsystematic order.[4]
(24) Cf. R. A. Marcus and N. Sutin, *Inorg. Chem.*, **14**, 213 (1975), and earlier papers.
(25) R. S. Mulliken and W. B. Person, "Molecular Complexes, A Lecture and Reprint Volume", Wiley, New York, N.Y., 1969.
(26) (a) R. Foster, "Organic Charge Transfer Complexes", Academic Press, New York, N.Y., 1969, p 42ff. (b) The charge transfer contribution is minimal in the ground state of these complexes.
(27) The relationship is actually parabolic[26] and becomes linear at only small energy differences.
(28) For a discussion of bridging groups in inner-sphere electron transfer reactions see A. Haim, *Acc. Chem. Res.*, **8**, 264 (1975).
(29) (a) B. Grossman and A. Haim, *J. Am. Chem. Soc.*, **92**, 4835 (1970); (b) see also A. G. Sykes and R. N. F. Thorneley, *J. Chem. Soc. A*, 232 (1970).
(30) (a) V. S. Petrosyan, V. I. Bakhmutov, and O. A. Reutov, *J. Organomet. Chem.*, **72**, 79 (1974); (b) W. H. Puhl and H. F. Hennelke, *J. Phys. Chem.*, **77**, 558 (1973); (c) H. J. Emeleus and J. J. Lagowski, *J. Chem. Soc.*, 1497 (1959); 2484 (1963).
(31) H. Sadek and R. M. Fuoss, *J. Am. Chem. Soc.*, **72**, 301 (1950).
(32) The number 1.2 is derived from the data in Table V by taking into account $2IrCl_6^{2-}$ for each isobutylene formed; see eq 4.

Metallointercalation Reagents. Synthesis, Characterization, and Structural Properties of Thiolato(2,2′,2″-terpyridine)platinum(II) Complexes

K. W. Jennette, J. T. Gill, J. A. Sadownick, and S. J. Lippard*

Contribution from the Department of Chemistry, Columbia University, New York, New York 10027. *Received February 23, 1976*

Abstract: The synthesis, characterization, and x-ray crystal structure analysis of 2-hydroxyethanethiolato(2,2′,2″-terpyridine)-platinum(II) nitrate, $[Pt(terpy)(SCH_2CH_2OH)]NO_3$, are reported. Solution studies reveal the presence of both monomers and stacked dimers in aqueous media above 10^{-4} M. The red complex crystallizes in the triclinic space group $P\bar{1}$ with two formula units per unit cell of dimensions a = 10.487 (2) Å, b = 10.718 (2) Å, c = 9.131 (2) Å, α = 82.72 (1)°, β = 111.96 (1)°, and γ = 112.53 (1)°. From 3224 unique observed reflections collected on an automated four-circle diffractometer, the structure was solved and refined to final values for the discrepancy indices of R_1 = 0.028, R_2 = 0.033. The platinum in the slightly distorted square planar complex is bound to the three nitrogen atoms of terpyridine and to the sulfur atom of mercaptoethanol with N–Pt–N angles of 80.6 (2) and 80.8 (2)° and N–Pt–S angles of 100.4 (1) and 98.1 (2)°. The Pt–N bond to the middle nitrogen atom of the terpyridine ligand is shorter, 1.968 (5) Å, than those to the other nitrogen atoms, 2.023 (5) and 2.030 (5) Å. The two methylene carbon atoms of the mercaptoethanol ligand are disordered. There is a hydrogen bond between the hydroxyl proton on the mercaptoethanol ligand and an oxygen atom of the nitrate anion. Two types of stacking interactions are seen in the crystal, a direct head-to-tail overlap, and an overlap involving only two of the three aromatic rings of the terpyridine ligand. A comparison is made of the stacking properties of $[Pt(terpy)(SCH_2CH_2OH)]NO_3$ with those of ethidium bromide. Both compounds are known to bind to double stranded DNA by intercalation. The syntheses and preliminary characterization of several related metallointercalation reagents in the class $[Pt(terpy)(SCH_2R)]^{n+}$ are reported.

The use of electron dense metal ions or complexes as probes for elucidating biological structure and function is of great interest.[1-4] We recently found that the heavy metal complex 2-hydroxyethanethiolato(2,2′,2″-terpyridine)-platinum(II), $[Pt(terpy)(HET)]^+$, binds strongly to DNA by intercalation.[5] This metallointercalation reagent is an example of an "addition probe"[1] that facilitates the study of the intercalator–nucleic acid complex.

The intercalation mechanism for binding of planar aromatic dyes to DNA was first suggested by Lerman.[6] He proposed that the flat portion of a dye molecule inserts between adjacent base pairs in the DNA double helix. The base pairs, which remain perpendicular to the helix axis, move apart 3.4 Å to accommodate the intercalator. The DNA-dye intercalation complex is stabilized by hydrophobic, polar, and dipolar interactions, and by the electrostatic forces of the cationic dye with the polyanionic nucleic acid. X-Ray fiber diffraction patterns[6-8] of intercalation complexes of various acridines and ethidium with DNA show loss of regular helical structure, a decrease in the helix diameter, and retention of the 3.4 Å spacing of the base pairs. The strong intercalative binding of many dyes is restricted to one binding site per 2–2.5 base pairs. Cairns[9] measured an approximate 44% lengthening of T2 DNA containing bound proflavine and suggested that only every second site between base pairs is available for intercalation. This nearest "neighbor exclusion" binding model proposes that intercalation of a dye at a given site prevents binding at an adjacent site,[10] giving rise to bound intercalator at every other interbase pair site at saturation. Among the types of drug molecules known to intercalate are antibiotics, antibacterials, trypanocides, antimalarials, schistosomicides, antitumor substances, and mutagens.[11]

Platinum and palladium terpyridine compounds were first synthesized by Morgan and Burstall[12] and later investigated by several workers.[13-15] Initial studies of the binding of $[Pt(terpy)Cl]^+$ to calf thymus DNA revealed covalent interactions with the bases, as well as intercalation.[5] In order to prevent binding to the bases, derivatives of $[Pt(terpy)Cl]^+$ were synthesized by substituting the relatively labile chloride with a sulfur donor ligand. The rate of substitution of the Pt–S bond is expected to be several orders of magnitude slower than the Pt–Cl bond.[16] This approach proved to be satisfactory, and extensive studies of the interaction of 2-hydroxyethanethiolato(2,2′,2″-terpyridine)platinum(II), $[Pt(terpy)(HET)]^+$ (Figure 1), with DNA showed that it binds strongly by intercalation.[5]

The utility of this electron dense metallointercalation reagent was subsequently demonstrated in x-ray fiber diffraction studies of $[Pt(terpy)(HET)]^+$ bound to DNA.[17] The fiber patterns retain the strong 3.4 Å meridional reflection from the stacked base pairs. The equatorial reflections revealed the effective molecular diameter, d_{eff}, to be 24 Å at 92% relative humidity. This value is smaller than that of B-DNA, 25 Å, and is remarkably similar to the d_{eff} of DNA containing bound ethidium bromide, Etd Br, 23.9 Å. In addition, near-meridional reflections appeared on 10.2 and 5.1 Å layer lines. These re-

flections are absent from previously published fiber diffraction patterns of DNA containing intercalated proflavine or ethidium.[6-8] The neighbor exclusion model requires a chemical repeat unit of one dye and two base pairs giving a spacing of 3×3.4 Å, 10.2 Å. The presence of the heavy platinum atom in the intercalator, with almost twice as many electrons as a base pair or organic intercalator, enhances the electron density at a 10.2 Å periodicity and provides strong support for the neighbor exclusion model. Loss of regular helical structure in the DNA backbone is indicated by the loss of well-resolved inner layer lines with spacings >10.2 Å.

The present paper describes the properties of metallointercalation reagents in the class $[Pt(terpy)(SCH_2R)]^{n+}$. The characterization of these compounds is important, if not essential, in understanding their binding to DNA. Aggregation of intercalating dyes is a well-known phenomenon.[18-21] The tendency of platinum terpyridine complexes to aggregate was therefore studied. Most intercalators stack in their solid state lattices. The x-ray crystal structure of $[Pt(terpy)(SCH_2CH_2OH)]NO_3$ was undertaken to determine its packing interactions. Although the structures of $[Pd(terpy)Cl]Cl$[14] and $Pt(bpy)Cl_2$,[22] recently shown to bind DNA by intercalation,[5b] are known and their stacking patterns can be studied, these compounds do not contain a ligand capable of hydrogen bonding. The presence of coordinated mercaptoethanol in $[Pt(terpy)(HET)]^+$ could influence the packing interactions because of its hydrogen bonding capability. Knowledge of the details of these interactions can facilitate interpretation of the x-ray fiber patterns of polynucleotides having bound $[Pt(terpy)(HET)]^+$.

Extensive studies with DNA have been carried out using organic intercalators in which the ring substituents were modified.[23] The synthetic route to $[Pt(terpy)(HET)]^+$ was used to prepare complexes having different coordinated thiolate ligands for study as metallointercalators. The synthesis of several new cationic terpyridineplatinum(II) complexes bonded to sulfur donor ligands containing different functional groups (Figure 1) is reported here. These cations provide a means of evaluating the effects of charge, polarity, and steric bulk on the intercalation process. Moreover, the fusion of two or more such intercalators using the organic chemistry of their functional groups affords a route to polyintercalators, in which the length and type of connecting chain can be systematically varied. A number of polyintercalating dyes were described during the preparation of the present manuscript.[24]

Experimental Section

Physical Measurements. Infrared spectra were recorded on a Perkin-Elmer 621 or 137 spectrometer calibrated with polystyrene film. Solid samples were examined as KBr pellets or Nujol mulls. Proton nuclear magnetic resonance spectra were obtained using a Varian Associates T-60, A-60A, or HA-100 spectrometer. The complexes were dissolved in acetonitrile-d_3 or deuterium oxide. Tetramethylsilane or H_2O was used as an internal standard, and in the latter case, a chemical shift from Me_4Si was approximated. Electronic spectra were recorded on a Cary 17 or Cary 118C spectrophotometer. Conductivities were measured at 25 °C using an Industrial Instruments Inc. RC-16B2 or a Beckman RC-18A conductance bridge and a cell with platinized platinum electrodes. The cell constant was determined by standardization with 1.0 mM aqueous potassium chloride solution. Data were analyzed according to the method described by Feltham and Hayter.[25] Spectral grade nitromethane and deionized distilled water were used as solvents.

Preparations. Deionized distilled water was used in all cases. $[Pt(terpy)Cl]Cl\cdot 2H_2O$ and $[Pd(terpy)Cl]Cl\cdot 2H_2O$ were prepared according to the procedures of Morgan and Burstall[12] and Intille.[13] [Pt(terpy)Cl]Cl was converted to the nitrate salt by adding 2 equiv of silver nitrate and removing the precipitated silver chloride. This material, which probably contains water in the fourth coordination site, was not isolated and will be referred to as "platinum terpyridine nitrate". 2-Mercaptoacetaldehyde diethylacetal was prepared by a modification of a known procedure.[26] Other starting materials were commercially available. Microchemical analyses were performed by Galbraith Laboratories, Knoxville, Tenn.

2-Hydroxyethanethiolato(2,2′,2″-terpyridine)platinum(II) Nitrate, $[Pt(terpy)(SCH_2CH_2OH)]NO_3$, $[Pt(terpy)(HET)]NO_3$. A solution of 0.68 g of silver nitrate in 5 ml of water was added to 1.07 g of [Pt(terpy)Cl]Cl in 100 ml of water and stirred overnight. After removal of the silver chloride precipitate, the solution was evaporated to 25 ml. 2-Mercaptoethanol (0.2 ml) was added with stirring to the solution under nitrogen. The solution was brought to pH 5 with ~1 ml of 1.0 N sodium hydroxide and filtered. Filtration and subsequent steps were performed in the air. The complex was precipitated from the filtrate with ~200 ml of 3:1 acetone:ethyl ether, redissolved in a minimum amount of methanol, filtered, and precipitated with ethyl ether. The product was filtered and washed with ethyl ether. The yield was 0.8 g (70% based on Pt).

Anal. Calcd for $C_{17}H_{16}N_4O_4SPt$: C, 36.0; H, 2.84; N, 9.87; S, 5.65. Found: C, 35.8; H, 2.77; N, 9.77; S, 5.63.

Ir (KBr pellet): 3310, 3060 (sh), 3030, 2960, 2930, 2860 (w), 1735 (w), 1600 (s), 1580, 1492 (w), 1476 (s), 1453 (s), 1383 (s), 1332, 1315 (s), 1285 (w), 1270 (w), 1250 (w), 1210 (w), 1168 (w), 1134, 1116 (w), 1098 (w), 1044 (s), 1027, 1007, 980 (sh), 822, 780 (s), 718 (w), 692, 653 (w), 638 (w), 452 (w), 428 (w), 357 (w), 340 (sh,w) cm^{-1}.

2-Hydroxyethanethiolato(2,2′,2″-terpyridine)platinum(II) Hexafluorophosphate, $[Pt(terpy)(SCH_2CH_2OH)]PF_6$, $[Pt(terpy)(HET)]PF_6$. 2-Mercaptoethanol (0.12 ml) was added to 0.535 g of [Pt(terpy)Cl]Cl in 10 ml of water. After stirring for 2–3 min, a solution of 0.34 g of sodium hexafluorophosphate in ~5 ml of water was added. The product was filtered and washed with cold water, dissolved in acetone, and evaporated to half volume. The purple product was filtered and washed with ether. The yield was 0.41 g (63%).

Anal. Calcd for $C_{17}H_{16}N_3OF_6PSPt$: C, 31.4; H, 2.48; N, 6.46; S, 4.93; P, 4.76. Found: C, 31.3; H, 2.48; N, 6.34; S, 4.46; P, 4.69.

Ethanethiolato(2,2′,2″-terpyridine)platinum(II) Hexafluorophosphate, $[Pt(terpy)(SCH_2CH_3)]PF_6$, $[Pt(terpy)(ET)]PF_6$. Ethanethiol (0.15 ml) was added to 0.535 g of [Pt(terpy)Cl]Cl in 10 ml of water. After stirring for 3 min, a solution of 0.34 g of sodium hexafluorophosphate in ~5 ml of water was added to the reaction mixture. The purple solid was filtered and washed with cold water. The product was dried in vacuo over P_2O_5. The yield was 0.47 g (74%).

Anal. Calcd for $C_{17}H_{16}N_3F_6PSPt$: C; 32.2; H, 2.54; N, 6.62; S, 5.05. Found: C, 32.4; H, 2.50; N, 6.43; S, 4.06.

Ir (KBr pellet): 3100, 2960 (sh), 2925, 2860 (w), 1730 (w), 1606 (s), 1571, 1478 (s), 1451 (s), 1398 (s), 1316 (s), 1290 (w), 1255 (sh), 1245, 1165 (w), 1132 (w), 1115 (w), 1099 (sh), 1090 (sh), 1048 (w), 1025, 835 (s), 770 (s), 736 (w), 718 (w), 690 (w), 650 (w), 638 (w), 555 (s), 450 (w), 355 (w), 330 (w) cm^{-1}.

Formylmethanethiolato(2,2′,2″-terpyridine)platinum(II) Hexafluorophosphate, $[Pt(terpy)(SCH_2CHO)]PF_6$, $[Pt(terpy)(FMT)]PF_6$. 2-Mercaptoacetaldehyde diethylacetal (0.4 ml) was added to a solution of 0.25 g of platinum terpyridine nitrate in 20 ml of water. The mixture was stirred under nitrogen for 2–5 min and filtered. Filtration and subsequent steps were performed in the air. Acetone (150 ml) was added to the filtrate and the complex was precipitated with diethyl ether, filteredand washed several times with ether, dissolved in a minimum amount of water, and filtered. Potassium hexafluorophosphate (0.3 g) dissolved in 5 ml of water was added to the filtrate. The precipitated hexafluorophosphate salt of the complex was filtered, washed with water, dissolved in a small amount of acetone, and chromatographed on Whatman CF11 cellulose, eluting with acetone. The first fraction was collected and evaporated. The red precipitate was washed with ether and dried in vacuo over P_2O_5. The yield was 0.15 g (46%). The complex can be recrystallized from acetone.

Anal. Calcd for $C_{17}H_{14}N_3OF_6PSPt$: C, 31.5; H, 2.18; N, 6.48; S, 4.94. Found: C, 30.8; H, 2.21; N, 6.84; S, 5.16.

Carboethoxymethanethiolato(2,2′,2″-terpyridine)platinum(II) Hexafluorophosphate, $[Pt(terpy)(SCH_2CO_2CH_2CH_3)]PF_6$, $[Pt(terpy)(CMT)]PF_6$. Ethyl thioglycolate (0.2 ml) was added to a solution of 0.54 g of platinum terpyridine nitrate in 20 ml of water and stirred under nitrogen. The solution was brought to pH 5 with 1.0 N NaOH and filtered. The complex was precipitated from the filtrate with 250 ml of a 3:2 solution of diethyl ether:acetone, filtered, washed with ether, dissolved in a minimum quantity of water, and filtered. Initial filtration and subsequent steps were performed in the air. Potassium hexafluorophosphate (0.28 g) dissolved in a minimum amount of water

was added to the filtrate and the PF_6^- salt of the complex was precipitated. This was filtered, washed with water then diethyl ether, and dried in vacuo over P_2O_5. The yield was 0.45 g (65%). The complex is easily crystallized from acetonitrile, forming red needles.

Anal. Calcd for $C_{19}H_{18}N_3O_2F_6PSPt$: C, 33.0; H, 2.62; N, 6.07; S, 4.63. Found: C, 32.9; H, 2.57; N, 5.90; S, 4.80.

Ir (KBr pellet): 3100, 3020 (sh), 1715 (s), 1610 (s), 1585, 1482 (s), 1456 (s), 1403, 1374, 1322 (s), 1278 (s), 1222 (w), 1197 (w), 1175, 1145, 1128 (s), 1061, 1034 (s), 1000 (w), 838 (s), 780 (s), 750, 744, 728, 697 cm^{-1}.

2-Ammonioethanethiolato(2,2′,2″-terpyridine)platinum(II) Hexafluorophosphate, $[Pt(terpy)(SCH_2CH_2NH_3)](PF_6)_2$, [Pt(terpy)(AET)]$(PF_6)_2$. Platinum terpyridine nitrate (0.37 g) dissolved in 8 ml of water was combined with 0.20 g of 2-aminoethanethiol hydrochloride dissolved in 4 ml of water and stirred under nitrogen. Sodium hydroxide (1.0 N) was added dropwise to adjust the pH to 5–6. The solution was filtered; the complex was precipitated from the filtrate with acetone, filtered, dissolved in a minimum amount of water, and filtered. Initial filtration and subsequent steps were performed in the air. Potassium hexafluorophosphate (0.35 g) dissolved in a minimum quantity of water was added to the filtrate. The complex was filtered, washed with water, and dried in vacuo over P_2O_5. The yield was 0.28 g (54%).

Anal. Calcd for $C_{17}H_{18}N_4F_{12}P_2SPt$: C, 25.7; H, 2.28; N, 7.04; S, 4.03. Found: C, 25.2; H, 2.07; N, 6.94; S, 3.16.

Collection and Reduction of X-Ray Data. Crystals of [Pt(terpy)(HET)]NO_3 suitable for x-ray study were obtained by vapor diffusion of diethyl ether into a methanol solution of the compound. The complex crystallized as dark red prisms, several of which were mounted for study in Lindemann glass capillary tubes. One crystal was mounted exactly along $[0\bar{2}1]$ for preliminary study. Precession photographs taken with Cu $K\bar{\alpha}$ radiation showed the Laue symmetry to be $\bar{1}$. The space group $P\bar{1}$ was assumed, a choice that appears to be justified based on the successful refinement of the structure.

The crystal used for data collection was an irregular prism with 13 bounding faces, with approximate dimensions 0.17 × 0.15 × 0.12 mm. It was mounted approximately along $[\bar{2}13]$. Data were collected using a Picker FACS-1-DOS diffractometer. Using graphite monochromatized Mo $K\alpha_1$ (λ 0.709 26 Å) radiation, 25 reflections were centered, 12 of which were used to compute an orientation matrix and lattice parameters for data collection. The full set of 25 reflections was later refined by a least-squares method[27] to yield the following unit cell constants: a = 10.487 (2), b = 10.718 (2), c = 9.131 (2) Å; α = 82.72 (1), β = 111.96 (1), and γ = 112.53 (1)°. This cell is reduced and was used in all subsequent calculations. A systematic search using TRACER[27] revealed no higher symmetry. The conventional reduced cell parameters are a = 9.131 Å, b = 10.487 Å, c = 10.718 Å, α = 67.47°, β = 82.72°, and γ = 68.04°.

The calculated density for two formula units per cell is 2.144 g/cm^3, which agrees with the value of 2.16 (1) g/cm^3 measured by suspension in a mixture of $CBrCl_3$ and $CHBr_3$.

A total of 5093 reflections, $\pm h \pm k \pm l$ for $4° < 2\theta \leq 30°$ and $h \pm k \pm l$ for $30° < 2\theta \leq 55°$, were taken at 23 ± 1°. The 2θ scan width used was 2.0°, plus a correction for $K\alpha_1$–$K\alpha_2$ separation. The scan rate was 1°/min. The takeoff angle (TOA) at the x-ray tube was 2.0°, which gave about 80% of maximum intensity. The mosaic spread at TOA = 2.3° was measured by open counter ω scans of several strong reflections. The full-width at half maximum ranged from 0.10 to 0.13°. A 6.3 × 6.3 mm aperture was positioned in front of the scintillation counter about 31 cm from the crystal. Stationary-crystal, stationary-counter 20-s background counts were recorded at both the beginning and end of each scan. Three standard reflections, $(\bar{1}41)$, $(21\bar{3})$, and $(\bar{4}43)$, were monitored after every 97 data points. These showed random fluctuations of ±5% or less for which no correction was made.

The data were reduced in the usual manner, using a value of 0.04 for ϵ.[28,29] An absorption correction was applied.[27] Using the computed linear absorption coefficient[30] of 85.5 cm^{-1}, the calculated transmission coefficients ranged from 0.365 to 0.506. A total of 876 equivalent (hkl) and $(\bar{h}\bar{k}\bar{l})$ pairs were averaged to an agreement factor

$$\left(\sum_{i=1}^{876}\sum_{j=1}^{2}\left|\overline{F_i^2} - F_{ij}^2\right|\right) \Big/ \sum_{i=1}^{876}\overline{F_i^2}$$

of 0.015. The data were placed on an approximately absolute scale using a modification of Wilson's method.[27,31] The 3224 reflections for which $F^2 > 3\sigma(F^2)$ were used in the refinement of the structure.

Determination and Refinement of the Structure. A sharpened Patterson map was computed and solved for the position of the platinum atom. Isotropic refinement with only the platinum atom gave discrepancy factors[32] of R_1 = 0.186 and R_2 = 0.261. A difference Fourier map at this stage revealed the location of all atoms except the hydrogens and carbon atoms of the mercaptoethanol ligand. Using neutral atom scattering factors,[33] isotropic refinement of the platinum, sulfur, 4 nitrogen, 4 oxygen, and 15 carbon atoms with unit weights resulted in discrepancy factors of R_1 = 0.096 and R_2 = 0.134. A difference Fourier map at this point revealed the presence of several peaks in the region expected for the carbon atoms of the mercaptoethanol ligand. A careful examination of the electron density suggested that the ethylene carbon chain resides in two orientations of partial occupancy of about 50% each. Four carbon atoms were therefore introduced with initial multipliers of 0.5. Refinement was then carried out using anisotropic thermal parameters and a variable methylene carbon atom multiplier which constrained the total occupancy of the two chemically reasonable ethylene chains to be 1.0. A difference Fourier map was then calculated and all the hydrogen atoms except those in the disordered ethylene chain were located. The bond distances to two carbon atoms in the mercaptoethanol tail were distorted owing to the close proximity of these atoms as indicated on electron density maps. Various refinements were undertaken to remedy this, including rigid-body refinements with fixed C–C–O and C–C–S groups, and refinement of the rigid C–C–S group with fixed oxygen positions. Since none of these gave completely standard bond lengths, the final refinement used isotropic thermal parameters for the four carbon atoms of the mercaptoethanol group and for the terpyridine and hydroxyl hydrogen atoms, and anisotropic thermal parameters for all other atoms. The multipliers for the two positions of the mercaptoethanol carbon atoms were 0.46 and 0.54.

This refinement, based on a total of 291 variable parameters, converged at R_1 = 0.028 and R_2 = 0.033. Inspection of the function $w\Delta^2$ for reflections ordered according to $|F_o|$ and $(\sin\theta)/\lambda$ showed satisfactory consistency, and the value of the standard deviation of an observation of unit weight was 0.96. The weighting scheme was therefore deemed to be adequate.[34] A final difference Fourier map showed three residual electron density peaks in the vicinity of the platinum atom between 0.89 and 1.18 e/Å^3, and one peak near the sulfur atom of 1.19 e/Å^3. All other peaks had electron density ≤0.67 e/Å^3 on a scale where a typical value for carbon was 6.5 e/Å^3

Results

Synthesis. The compounds shown in Figure 1 were prepared according to eq 1 and 2.

$$[Pt(terpy)Cl]^+ + Ag^+ \xrightarrow{H_2O} [Pt(terpy)(OH_2)]^{2+} + AgCl \quad (1)$$

$$[Pt(terpy)(OH_2)]^{2+} + HSR + OH^-(\text{to pH } 5\text{–}6) \rightarrow [Pt(terpy)(SR)]^+ + 2H_2O \quad (2)$$

The silver ion must be thoroughly removed from the platinum terpyridine nitrate in the first step. The best results were obtained when the product was isolated as quickly as possible after the addition of the mercaptan ligand. The pH must be carefully adjusted during the second step, since the complexes are unstable to basic conditions. The second step was carried out under nitrogen. Isolation procedures after this step did not require anaerobic conditions.

Nuclear Magnetic Resonance. Proton nuclear magnetic resonance (NMR) spectral data for the terpyridineplatinum(II) complexes are summarized in Table I. The labeling scheme for the protons is shown in Figure 1. The proton NMR spectra of [Pt(terpy)Cl]Cl, [Pt(terpy)$(SCH_2CH_2OH)]NO_3$, and [Pt(terpy)$(SCH_2CHO)]PF_6$ are shown in Figure 2. Assignments follow those previously published,[35] and were aided by large coupling constants due to the 33.8% abundant ^{195}Pt isotope which has I = ½. The doublet farthest downfield in the spectrum of [Pt(terpy)(HET)]NO_3 shows platinum coupling

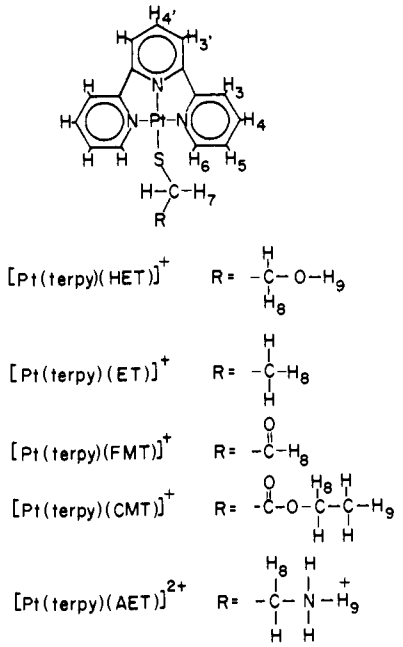

Figure 1. Platinum terpyridine thiolate complexes showing the NMR labeling scheme and ligand abbreviations.

and is assigned as H_6. The chemical shift of this resonance is approximately constant among the thiolate complexes studied, but appears 0.8–1.7 ppm farther upfield in the spectra of [Pt(terpy)Cl]Cl and [Pt(terpy)H_2O]$(NO_3)_2$. Proton H_6 is coupled to H_5 ($J_{H_5-H_6}$ = 5.5 Hz), and the small (~1–2 Hz) additional splittings of each peak of the doublet indicate long range coupling to protons H_3 and H_4. The triplet at δ ~7.6 ppm corresponds to the H_5 proton, and the remaining large, complicated multiplet is assigned to the rest of the terpyridine ring protons. The H_5 resonance integrates for two protons, and decoupling of the H_6 protons causes collapse of the triplet into the expected doublet.[36] The resonances of the coordinated thiolate ligands are readily assigned since platinum coupling to the H_7 protons is apparent and the chemical shifts and coupling constants of the other protons are those expected for the particular functional group. The hydroxyl proton of [Pt(terpy)(HET)]PF_6 was identified at δ 2.70 ppm since it coalesced with water when D_2O was added to the CD_3CN solution.

The chemical shifts in Table I are both solvent and concentration dependent. The entire spectrum of [Pt(terpy)Cl]Cl moves upfield as the concentration is increased from 0.01 to 0.07 M, with the H_6 resonance moving farther than the others.

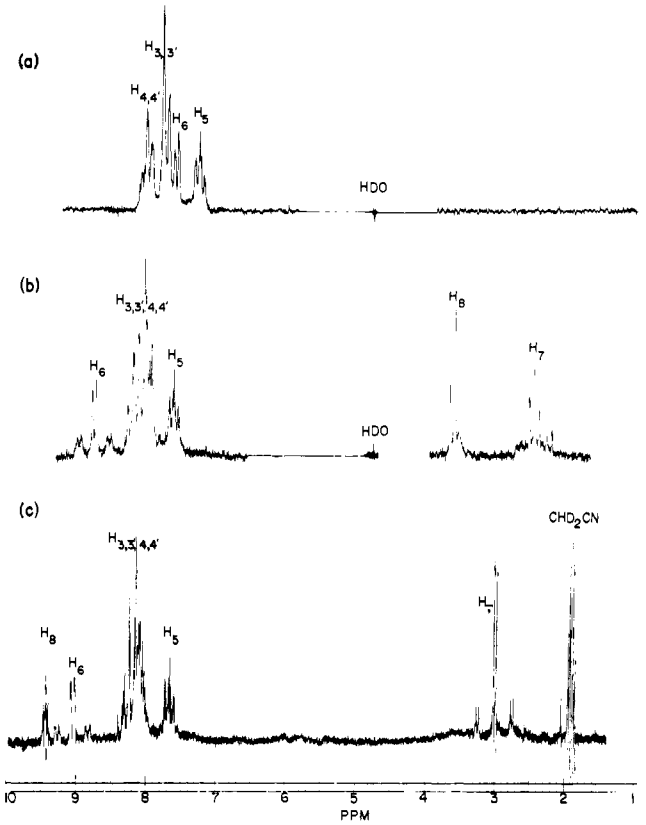

Figure 2. The 100-MHz proton magnetic resonance spectra of (a) [Pt(terpy)Cl]Cl in D_2O in parts per million from Me_4Si at 60 °C, (b) [Pt(terpy)(HET)]NO_3 in D_2O in parts per million from Me_4Si at 30 °C, and (c) [Pt(terpy)(FMT)]PF_6 in acetonitrile-d_3 in parts per million from internal Me_4Si at 30 °C.

Similar upfield shifts are evident when the spectrum of [Pt(terpy)(HET)]PF_6 in CD_3CN is compared to that of [Pt(terpy)(HET)]NO_3 in D_2O. Extensive stacking of terpyridineplatinum(II) cations is more favored in concentrated than dilute aqueous solutions, while nonaqueous solvents minimize stacking (vide infra).

For each of the thiolate ligands of Table I bonded to terpyridineplatinum(II), the chemical shift difference between the H_6 and H_5 resonances is of nearly constant magnitude. Although its origin is uncertain, this effect may result in part from close nonbonding hydrogen–hydrogen contacts.[35] There are three such close intramolecular nonbonded contacts (2.55, 2.56, and 2.59 Å, compared with the sum of van der Waals hydrogen radii[37] of 2.4 Å) between positions calculated for the

Table I. Proton Nuclear Magnetic Resonance Chemical Shifts (δ) and Coupling Constants for [Pt(terpy)L]X Complexes[a]

L	X	Solvent	$H_{3,3',4,4'}$	H_5	H_6	H_7	H_8	H_9	$J_{H_5-H_6}$	J_{H_6-Pt}	J_{H_7-Pt}	$J_{H_7-H_8}$
$-SCH_2CH_2OH$[b]	NO_3^-	D_2O	8.01[c]	7.60	8.74	2.44	3.58		5.5	44	38	7.0
$-SCH_2CH_2OH$	PF_6^-	CD_3CN	8.19	7.68	9.16	2.48	3.57	2.70	5.5	45	39	7.0
$-SCH_2CH_3$	PF_6^-	CD_3CN	8.17	7.69	9.16	2.43	1.27		5.5	45	43	7.0
$-SCH_2C(=O)H$	PF_6^-	CD_3CN	8.12	7.68	9.04	2.99	9.42		5.5	43	49	3.5
$-SCH_2C(=O)OCH_2CH_3$	PF_6^-	CD_3CN	8.30	7.77	9.22	3.06	3.90	1.00	5.5	44	48	7.0[d]
$-SCH_2CH_2NH_3^+$	$2PF_6^-$	CD_3CN	8.14	7.68	8.94	2.54	3.04	4.58[e]	5.5	43	42	6.5
Cl^-	Cl^-	D_2O	7.99[f]	7.47	7.99							
			7.77[g]	7.24	7.57							
H_2O	$2NO_3$	D_2O	8.06	7.53	7.99							

[a] Data in D_2O solutions are in parts per million from Me_4Si, converted using the value of 4.75 ppm for the chemical shift difference between HDO and Me_4Si; data in CD_3CN solutions are in parts per million from tetramethylsilane. The labeling is shown in Figure 1. J = coupling constant in hertz. Data were obtained at 30 °C from 100-MHz spectra. [b] Saturated solution; these chemical shifts are concentration dependent. [c] Multiplet with at least eight well-defined resonances; chemical shift given refers to position of most intense peak of this multiplet, probably the lowfield peak of the H_3 doublet. [d] $J_{H_8-H_9}$. [e] Broad. [f] 0.01 M. [g] 0.07 M. This spectrum was taken at 60 °C to improve the resolution. Chemical shift values (δ) increased 3 Hz for H_5 and 5 Hz for H_6 upon heating from 30 to 60 °C.

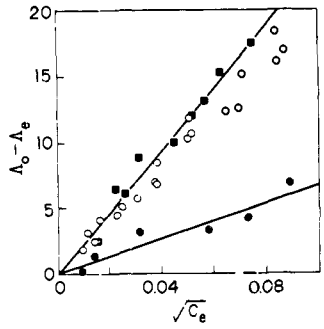

Figure 3. Conductivities ($\Lambda_0 - \Lambda_e$, in ohm^{-1} cm^2 equiv^{-1}) of ○, [Pt(terpy)(HET)]NO_3 (slope = 212); ■, [Pt(py)$_2$(en)](ClO_4)$_2$ (slope = 238, solid line); and ●, KCl (slope = 70, solid line) plotted as a function of $\sqrt{C_e}$.

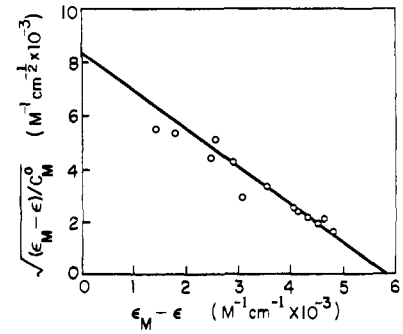

Figure 4. Plot to determine the dimerization constant of [Pt(terpy)(HET)]NO_3 in aqueous solution using the 342-nm band. Concentrations ranged from 4.7×10^{-5} to 1.8×10^{-3} M. Symbols are defined in the text.

methylene hydrogens of the 2-hydroxyethanethiolate ligand and the terpyridine H1 atom in the structure of [Pt(terpy)(HET)]NO_3. This result suggests that the methylene hydrogens of the thiolate ligands in Table I may deshield H_6. A more important factor in the deshielding of H_6, however, is likely to be the magnetic anisotropy of the platinum-sulfur bond. Downfield shifts of protons near carbon-sulfur double bonds have been reported in cyclic amine *N*-carbodithioic acid salts,[38a] thionocarbamates,[38b,c] and thiazoline thiones.[38d] For a selection of platinum(II) bipyridine[39] and terpyridine complexes (Table I), the downfield shift of the H_6 resonance from that of H_5 decreases as the remaining ligand(s) are varied in the following order: RS^- (~120 Hz) > NR_3 (~85 Hz) > H_2O ~ Cl^- (~40 Hz). There is a corresponding decrease in the polarizability of the above ligands, implicating an electronic factor in the deshielding of H_6. Whatever the source, however, the downfield shift of the H_6 resonance with respect to that of H_5 is useful for identifying sulfur (vs. water or chloride) coordination to terpyridineplatinum(II).

Conductance Measurements. The conductivities of [Pt(terpy)(HET)]$^+$ and several reference electrolytes are shown in Figure 3. The data are plotted according to the limiting Onsager law: $\Lambda_0 - \Lambda_e = B\sqrt{C_e}$, where Λ_e is the equivalent conductance, Λ_0 is the conductance extrapolated to zero concentration, C_e is the equivalent concentration, and B is the empirical slope. B is a term depending on Λ_0, the charges of the ions, dielectric constant and viscosity of solvent, temperature, and ionic mobilities, and, therefore, directly reflects the electrolyte type for the complex.[25,40,41] Comparison of the slope (212, accurate to ±10%) of [Pt(terpy)(HET)]$^+$ with those of 1:1 (KCl, slope = 70) and 2:1 ($BaCl_2$, slope = 183; [Pt(py)$_2$(en)](ClO_4)$_2$, slope = 238) electrolytes showed that over the concentration range of 10^{-4} to 10^{-2} M in aqueous solution, this metallointercalator behaves as a 2:1 electrolyte. In the organic solvent nitromethane, it is a 1:1 electrolyte (slope of [Pt(terpy)(HET)]PF_6 = 203, lit.,[25] 1:1 electrolyte, slope ~200). By comparison, the conductivity of [Pt(terpy)Cl]Cl in aqueous solution indicated that at concentrations above 10^{-3} M it was a 2:1 electrolyte (slope = 219), but at lower concentrations the conductivity sharply increased showing behavior typical of a weak electrolyte.

Electronic Spectroscopy. In very dilute aqueous solutions, ≤15 μM, the molar extinction coefficient of [Pt(terpy)(HET)]NO_3 was found to be independent of concentration. Maxima in the uv-visible spectrum are found at 475 nm (ε 875), 342 (12 500), 327 (10 700), 311 (10 500), 278 (19 300), and 242 (28 700). Upon increasing the concentration, however, the relative intensities and molar extinction coefficients of all the peaks changed, although their positions remained unaltered. This hypochromicity is due to the formation of a dimer which has a different spectrum than the monomer. The dimerization constant and the molar extinction coefficient of the dimer can be obtained from the equation $[(\epsilon_M - \epsilon)/C_M^0]^{1/2} = (2K_d/\Delta\epsilon)^{1/2}[\Delta\epsilon - (\epsilon_M - \epsilon)]$,[18] where ϵ, ϵ_M, and ϵ_D are the extinction coefficients of the solution, the pure monomer, and the pure dimer, respectively, C_M^0 is the concentration based on the molecular weight of the monomer unit, $\Delta\epsilon$ is $\epsilon_M - \epsilon_D$, and K_d is the equilibrium constant of dimerization. A plot of $[(\epsilon_M - \epsilon)/C_M^0]^{1/2}$ vs. $(\epsilon_M - \epsilon)$ yields a straight line with intercepts $(2K_d\Delta\epsilon)^{1/2}$ on the ordinate and $\Delta\epsilon$ on the abscissa. Figure 4 shows this plot for the 342-nm band of [Pt(terpy)(HET)]NO_3 in aqueous solution. With C_M^0 between 4.7×10^{-5} and 1.8×10^{-3} M, the dimerization constant varied depending on wavelength with $K_d = 6 \times 10^3$ M^{-1} at 342 nm, 12×10^3 M^{-1} at 311 nm, and 3×10^3 M^{-1} at 242 nm, averaging to $K_d = (7 \pm 5) \times 10^3$ M^{-1}.

The molar extinction coefficient of both [Pt(terpy)Cl]Cl and [Pd(terpy)Cl]Cl in aqueous solutions varied with concentration above 1 μM. In 0.05 M Tris·HCl, pH 7.5, 0.1 M NaCl, however, [Pt(terpy)Cl]Cl followed Beer's law at concentrations below 15 μM, with defined spectral maxima (and molar extinction coefficients) at 343 (11 300), 327 (12 600), 278 (25 100), and 248 (28 800) nm. The dimerization constant for [Pt(terpy)Cl]Cl in water obtained by the method described above using 343- and 327-nm bands with C_M^0 between 3.0×10^{-5} and 1.0×10^{-3} M averaged $(4 \pm 2) \times 10^3$ M^{-1}.

X-Ray Structural Results for [Pt(terpy)(SCH$_2$CH$_2$OH)]NO_3. The final positional, thermal, and (for mercaptoethanol carbon atoms) occupancy parameters, with their standard deviations derived from the inverse matrix of the final least-squares refinement cycle, are reported in Table II. The pertinent interatomic distances and angles and their standard deviations are summarized in Table III. Table IV contains the results of best-plane and dihedral angle calculations. The root-mean-square amplitudes of thermal vibration for all anisotropically refined atoms, Table V, and Table VI, listing the final observed and calculated structure factor amplitudes, are available.[42]

Figure 5 shows a drawing of the molecule and the atom-labeling scheme. The two types of stacking interactions are displayed in Figure 6, and Figure 7 portrays the packing of the molecules within and about one unit cell.

Discussion

Molecular Geometry of [Pt(terpy)(SCH$_2$CH$_2$OH)]NO_3. The cation consists of platinum coordinated to the tridentate terpyridine ligand and to the sulfur atom of the mercaptoethanol ligand, as shown in Figure 5. The coordination geometry is essentially square planar with distortions arising from the constraints of the terpyridine ligand. The maximum deviation of the platinum, sulfur, and three nitrogen atoms from the best plane through all five atoms is 0.013 Å (Table IV). The Pt–N distance to the middle nitrogen atom (N2) of the terpyridine ligand, 1.968 (5) Å, is slightly shorter than the distances of platinum to the other two nitrogen atoms, N1, 2.023 (5) Å, and

Table II. Final Positional, Thermal, and Occupancy Parameters of the Atoms of $[Pt(terpy)(SCH_2CH_2OH)]NO_3$[a,b]

Atom	x	y	z	β_{11}[c] or B[d]	β_{22}[c] or O.F.[e]	β_{33}	β_{12}	β_{13}	β_{23}
Pt	−0.04171 (2)	0.06775 (2)	−0.19384 (3)	11.43 (3)	7.78 (2)	13.33 (4)	4.35 (2)	5.59 (2)	0.42 (2)
S	−0.2770 (2)	0.0485 (2)	−0.2259 (3)	12.9 (2)	14.9 (2)	25.6 (3)	6.7 (2)	5.6 (2)	−3.3 (2)
O1	−0.3867 (10)	0.3520 (8)	−0.4839 (10)	33.6 (16)	17.3 (9)	27.7 (15)	11.6 (10)	16.5 (13)	3.5 (9)
O2	−0.2281 (6)	0.3257 (6)	0.1172 (8)	20.7 (9)	14.1 (7)	34.5 (14)	5.4 (6)	7.6 (9)	−7.2 (8)
O3	−0.0896)7)	0.4957 (7)	0.2703 (8)	16.7 (8)	19.3 (9)	35.2 (14)	2.2 (7)	8.5 (9)	−9.6 (9)
O4	−0.3162 (7)	0.4148 (10)	0.2362 (8)	16.7 (9)	49.4 (21)	28.6 (14)	6.2 (11)	7.6 (9)	−14.6 (14)
N1	0.0790 (5)	0.2294 (4)	−0.0445 (5)	12.9 (6)	8.3 (5)	13.3 (7)	5.3 (5)	4.5 (5)	0.8 (5)
N2	0.1579 (5)	0.0815 (5)	−0.1693 (5)	12.4 (6)	9.5 (5)	13.1 (7)	5.1 (5)	5.6 (5)	0.5 (5)
N3	−0.0963 (6)	−0.0916 (5)	−0.3332 (6)	15.0 (7)	8.6 (5)	15.3 (8)	4.9 (5)	6.6 (6)	0.9 (5)
N4	−0.2104 (7)	0.4091 (7)	0.2110 (7)	15.0 (9)	14.6 (8)	19.7 (11)	5.9 (7)	5.6 (8)	0.3 (7)
C1	0.0311 (8)	0.2990 (6)	0.0225 (7)	14.0 (9)	9.7 (7)	13.6 (9)	5.4 (6)	5.4 (7)	−0.2 (6)
C2	0.1249 (8)	0.4033 (7)	0.1276 (8)	18.4 (11)	11.1 (7)	16.7 (11)	7.6 (8)	6.9 (9)	−0.3 (7)
C3	0.2747 (9)	0.4429 (8)	0.1642 (9)	18.9 (12)	11.5 (8)	15.7 (11)	5.3 (8)	3.8 (9)	−2.1 (8)
C4	0.3261 (8)	0.3711 (7)	0.0972 (8)	14.5 (10)	11.2 (8)	17.8 (11)	4.0 (7)	5.3 (8)	−1.9 (7)
C5	0.2279 (7)	0.2662 (6)	−0.0062 (7)	12.4 (8)	10.7 (7)	13.6 (9)	4.9 (6)	4.5 (7)	−0.2 (6)
C6	0.2732 (6)	0.1818 (6)	−0.0777 (7)	11.9 (7)	9.9 (6)	13.9 (9)	3.9 (6)	5.7 (7)	1.3 (6)
C7	0.4140 (8)	0.1947 (8)	−0.0601 (9)	12.4 (9)	14.0 (9)	19.2 (12)	4.7 (7)	7.2 (9)	0.4 (8)
C8	0.4306 (8)	0.0998 (8)	−0.1339 (9)	15.1 (10)	16.6 (10)	21.3 (13)	8.3 (9)	9.6 (9)	2.8 (9)
C9	0.3085 (9)	−0.0024 (8)	−0.2279 (9)	19.5 (11)	13.9 (9)	20.0 (12)	9.7 (9)	11.3 (10)	2.0 (8)
C10	0.1704 (7)	−0.0101 (6)	−0.2445 (7)	15.8 (9)	11.2 (7)	15.8 (10)	6.9 (7)	8.6 (8)	2.0 (7)
C11	0.0264 (7)	−0.1081 (6)	−0.3401 (7)	17.6 (9)	8.0 (6)	14.4 (9)	5.5 (6)	8.3 (8)	1.3 (6)
C12	0.0075 (10)	−0.2110 (7)	−0.4315 (8)	23.6 (13)	11.2 (8)	17.0 (11)	8.8 (9)	11.3 (10)	2.3 (7)
C13	−0.1311 (11)	−0.2977 (8)	−0.5158 (9)	28.8 (17)	10.0 (8)	18.0 (12)	6.6 (10)	9.6 (12)	−1.1 (8)
C14	−0.2528 (10)	−0.2819 (7)	−0.5066 (9)	21.5 (13)	9.6 (7)	16.5 (11)	3.1 (8)	5.8 (10)	−1.3 (7)
C15	−0.2315 (8)	−0.1776 (6)	−0.4165 (8)	16.4 (10)	9.1 (7)	15.8 (10)	3.8 (7)	4.8 (8)	−0.6 (7)
C161	−0.3516 (15)	0.1289 (14)	−0.3873 (16)	4.54 (39)[d]	0.46 (2)[e]				
C171	−0.2792 (21)	0.2775 (22)	−0.3556 (25)	5.89 (42)	0.46				
C162	−0.2718 (19)	0.2342 (19)	−0.2982 (24)	6.43 (40)	0.54				
C172	−0.3880 (20)	0.2222 (20)	−0.4573 (23)	7.56 (52)	0.54				
H1	−0.055 (7)	0.273 (6)	−0.001 (7)	1.5 (13)					
H2	0.093 (9)	0.446 (8)	0.170 (9)	3.8 (18)					
H3	0.334 (9)	0.502 (8)	0.248 (10)	3.9 (18)					
H4	0.419 (7)	0.387 (6)	0.123 (7)	1.9 (13)					
H7	0.492 (8)	0.257 (7)	0.001 (8)	2.6 (15)					
H8	0.521 (6)	0.103 (5)	−0.129 (6)	0.4 (9)					
H9	0.312 (7)	−0.066 (7)	−0.277 (8)	2.6 (14)					
H12	0.066 (12)	−0.245 (11)	−0.430 (12)	7.1 (29)					
H13	−0.145 (9)	−0.368 (9)	−0.576 (10)	5.1 (21)					
H14	−0.359 (10)	−0.354 (9)	−0.569 (10)	5.2 (21)					
H15	−0.318 (8)	−0.173 (7)	−0.400 (8)	2.6 (15)					
HO	−0.354 (11)	0.368 (10)	−0.530 (11)	3.6 (25)					

[a] Atoms are labeled as indicated in Figure 5. Hydrogens are labeled to correspond to the carbon atoms (or oxygen 1) to which they are attached. [b] Standard deviations, in parentheses besides each entry, occur in the last significant figure(s) for each parameter. [c] Anisotropic thermal parameters are of the form $\exp[-(\beta_{11}h^2 + \beta_{22}k^2 + \beta_{33}l^2 + 2\beta_{12}hk + 2\beta_{13}hl + 2\beta_{23}kl)]$; values reported are $\times 10^3$. [d] Isotropic thermal parameters. [e] Occupancy factors.

N3, 2.030 (5) Å. This pattern also occurs in the structure of $[Pd(terpy)Cl]Cl\cdot 2H_2O$,[14] where the one Pd-N bond to the center nitrogen atom, 1.96 (2) Å, is shorter than the other Pd-N distances, 2.10 (2) and 2.04 (2) Å, as well as in the five-coordinate complexes, $Co(terpy)Cl_2$[43] and $Zn(terpy)Cl_2$.[44] The Pt-N distances in *trans*-(dithiocyanato)bis(pyridine)platinum(II) are 2.041 (9) Å.[45] The N-Pt-N angles of 80.6 (2) and 80.8 (2)° in $[Pt(terpy)(HET)]NO_3$ are significantly smaller than the theoretical 90° values expected for a square complex. This effect is also seen in [Pd(terpy)Cl]Cl where these angles are 82 (2) and 79 (2)°. The Pt-N bond distance pattern and the N-Pt-N angles in $[Pt(terpy)(HET)]NO_3$ are significantly different than those found in the analogous nonaromatic compound [Pt(dien)Br]Br.[46] The Pt-N bond lengths in the latter are 1.96 (2), 1.98 (2), and 2.12 (2) Å and the N-Pt-N angles are 87.3 (7) and 83.4 (7)°. Although these angles are smaller than 90°, showing some strain in the chelate rings of the tridentate diethylenetriamine ligand, they are larger than those found in $[Pt(terpy)(HET)]^+$. This result indicates that the terpyridineplatinum(II) is somewhat more strained than the diethylenetriamine analogue, and may account for the 10^3-10^4 times higher reactivity of $[Pt(terpy)X]^+$ towards pyridine substitution compared with $[Pt(dien)X]^+$.[15]

The platinum-sulfur bond length of 2.303 (2) Å is comparable to the Pt-S distance of 2.322 (2) Å in *trans*-(dithiocyanato)bis(pyridine)platinum(II).[45] The N-Pt-S angles in $[Pt(terpy)(HET)]NO_3$ are 100.4 (1) and 98.1 (2)°, again reflecting the strain caused by the terpyridine chelation, and can be compared to the N-Pd-Cl angles in [Pd(terpy)Cl]Cl[14] of 96 (2) and 101 (2)°. The terpyridine ligand has internal bond distances and angles (Table III) expected for this system.[47] The best mean plane calculated through the platinum atom, sulfur atom, and terpyridine ligand shows some slight puckering of the pyridine rings, with C2 displaced by 0.111 (7) Å and all other atoms by less than 0.06 Å from that plane.

The nitrate anion is trigonal planar with O-N-O angles of 118.3 (7), 120.1 (7), and 121.4 (7)°. No atom deviates more than 0.025 (6) Å from a best plane through the four atoms. The N-O distances are 1.214 (8), 1.231 (8), and 1.239 (8) Å.

The plane through the nitrate anion makes an angle of 169.5 (4)° with that of platinum, sulfur, and terpyridine, showing they are almost coplanar.

Hydrogen Bonding and Disorder of the Mercaptoethanol

Table III. Interatomic Distances (Å) and Angles (deg)[a]

Coordination sphere		Terpyridine ligand			
Pt-S	2.303 (2)	N1-C1	1.347 (7)	C1-N1-C5	118.4 (5)
Pt-N1	2.023 (5)	N1-C5	1.368 (8)	C1-N1-Pt	128.4 (4)
Pt-N2	1.968 (5)	N2-C6	1.339 (7)	C5-N1-Pt	113.2 (4)
Pt-N3	2.030 (5)	N2-C10	1.338 (7)	C15-N3-C11	118.7 (5)
N1-Pt-N2	80.6 (2)	N3-C11	1.389 (8)	C15-N3-Pt	128.5 (5)
N2-Pt-N3	80.8 (2)	N3-C15	1.344 (8)	C11-N3-Pt	112.7 (4)
N1-Pt-S	100.4 (1)	C1-C2	1.364 (9)	C3-C4-C5	119.9 (7)
N3-Pt-S	98.1 (2)	C2-C3	1.375 (11)	C4-C5-N1	121.0 (6)
N1-Pt-N3	161.4 (2)	C3-C4	1.393 (10)	C4-C5-C6	123.4 (6)
N2-Pt-S	178.9 (9)	C4-C5	1.367 (9)	N1-C5-C6	115.6 (5)
		C5-C6	1.476 (8)	N2-C6-C7	119.1 (6)
Mercaptoethanol ligand		C6-C7	1.378 (9)	N2-C6-C5	112.6 (5)
		C7-C8	1.384 (10)	C5-C6-C7	128.3 (6)
		C8-C9	1.386 (11)	C6-C7-C8	118.3 (7)
S-C161	1.69 (1)	C9-C10	1.369 (9)	C7-C8-C9	120.8 (6)
S-C162	2.00 (2)	C10-C11	1.475 (9)	C8-C9-C10	119.0 (6)
C161-C171	1.49 (3)	C11-C12	1.376 (9)	C10-N2-C6	123.9 (5)
O1-C171	1.66 (2)	C12-C13	1.371 (12)	C10-N2-Pt	118.1 (4)
O1-C172	1.38 (2)	C13-C14	1.383 (12)	C6-N2-Pt	118.0 (4)
C162-C172	1.49 (3)	C14-C15	1.371 (10)	N1-C1-C2	122.7 (6)
S-C162-C172	108 (1)	C1-H1	0.79 (6)	C1-C2-C3	119.4 (7)
O1-C172-C162	103 (2)	C2-H2	0.85 (9)	C2-C3-C4	118.6 (7)
C161-S-Pt	112.6 (5)	C3-H3	0.92 (8)	N2-C10-C9	118.9 (6)
C162-S-Pt	100.9 (5)	C4-H4	0.87 (7)	N2-C10-C11	113.0 (5)
S-C161-C171	109 (1)	C7-H7	0.88 (7)	C9-C10-C11	128.1 (6)
HO-O1-C171	97 (10)	C8-H8	0.92 (5)	C12-C11-N3	119.7 (6)
HO-O1-C172	98 (10)	C9-H9	0.89 (7)	C12-C11-C10	125.0 (6)
O1-C171-C161	108 (1)	C12-H12	0.82 (11)	N3-C11-C10	115.3 (5)
		C13-H13	0.92 (9)	C11-C12-C13	120.8 (7)
		C14-H14	1.07 (9)	C12-C13-C14	119.2 (7)
Hydrogen bond		C15-H15	0.99 (7)	C13-C14-C15	119.1 (7)
				N3-C15-C14	122.5 (7)
O1-O4[b]	2.85 (1)			Nitrate anion	
O1-HO	0.61 (8)	O2-N4	1.231 (8)	O2-N4-O3	120.1 (7)
O4[b]-HO	2.27 (9)	O3-N4	1.214 (8)	O3-N4-O4	118.3 (7)
O1-HO-O4[b]	159 (12)	O4-N4	1.239 (8)	O2-N4-O4	121.4 (7)

[a] See footnotes *a* and *b*, Table II. Values reported here have not been corrected for thermal motion. [b] Atom at $x, y, z - 1.0$.

Ligand. In the crystal of $[Pt(terpy)(HET)]NO_3$, the hydroxyl proton on the mercaptoethanol arm is hydrogen bonded to O4* of the nitrate anion in a neighboring unit cell (Figure 7a). The O1···O4* distance is 2.85 (1) Å, the HO···O4* distance is 2.27 (9) Å, and the O1-HO-O4* angle is 159 (12)°. Although the sulfur atom is fixed through bonding to platinum, and the oxygen atom, which shows large thermal motion, by the hydrogen bond, the ethylene chain of the mercaptoethanol ligand has conformational freedom as manifest by the disorder found for its carbon atoms (Figure 5). The two positions of the mercaptoethanol ethylene group are approximately equally occupied. The positions of C162 and C171 are very close, and the overlap of electron density in this area causes distortions in the bond lengths and angles about these atoms to which we attribute no chemical significance. The conformational freedom of the mercaptoethanol tail and its ability to form a hydrogen bond probably occur in solution as well and perhaps in fibers in which $[Pt(terpy)(HET)]^+$ is bound to DNA by intercalation.[17] There are many types of interbase pair sites in DNA, and it is possible that the orientation of the $[Pt(terpy)(HET)]^+$ cation will be determined by the best hydrogen bonding arrangement for that particular site. Hydrogen bonding to the phosphates and to the bases is possible, if not likely, since in the $[Pt(terpy)(HET)]NO_3$ structure the oxygen atom of the mercaptoethanol tail is displaced by 3.5 Å from the plane of the platinum atom, sulfur atom, and terpyridine, while the hydrogen bonded nitrate oxygen atom is 5.87 Å away from that plane. When $[Pt(terpy)(HET)]^+$ intercalates into DNA, the mercaptoethanol tail may be in a position to hydrogen bond to the base pair or phosphate group next to the $[Pt(terpy)(HET)]^+$ site.

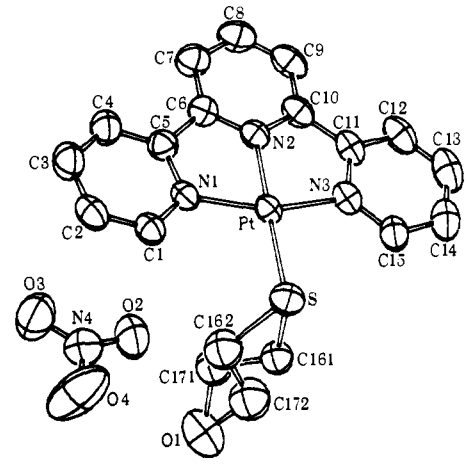

Figure 5. ORTEP drawing of the $[Pt(terpy)(HET)]NO_3$ molecule showing atom-labeling scheme and 50% probability thermal ellipsoids. The two positions for the disordered mercaptoethanol ethylene carbon chain are shown.

Stacking Intercations. Other likely forces governing the orientation of $[Pt(terpy)(HET)]^+$ intercalated into DNA are polar and dipolar interactions[48] of the planar, polarizable rings of terpyridine with those of the bases. The tendency to self-stack is indicative of an ability to intercalate. Intercalating

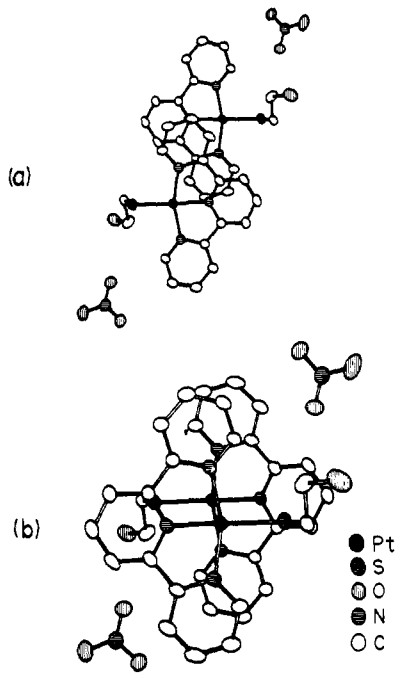

Figure 6. The two different stacking interactions, viewed normal to the planes of the terpyridine ligand, found in the structure of [Pt(terpy)(HET)]NO_3. Planes are seperated by 3.43 Å: (a) stacking with cation in adjacent unit cell, (b) within the unit cell.

reagents stack in solution as well as in crystalline form. Solution studies of $[Pt(terpy)(HET)]^+$ clearly show that it dimerizes in water over the concentration range of 10^{-4} to 10^{-2} M. Beer's law is not obeyed above 15 μM concentration, and the absorption changes give an equilibrium constant for dimerization of $(7 \pm 5) \times 10^3$ M^{-1}. The observed wavelength dependence of this value possibly reflects the presence of more than one stacked species in solution. Published dimerization constants for Etd Br are 30 M^{-1} in H_2O[20a] and 270 M^{-1} in 1.0 M NaCl,[20b] and that for proflavine is 500 M^{-1}.[18] NMR results also show that $[Pt(terpy)(HET)]^+$, $[Pt(terpy)Cl]^+$, and Etd^+ [19,20] aggregate in aqueous solution. The low dimerization constant of Etd Br may be a result of steric hindrance from the phenyl or ethyl substituents which are approximately perpendicular to the plane of the phenanthridinium ring system.

Table IV. Distances of Atoms from Best Planes and Dihedral Angle

Atoms defining best plane	Distance (Å) of atom from plane	Atoms defining best plane	Distance (Å) of atom from plane
	$-0.4547x - 6.006y + 6.852z = -1.716$[a]		
Pt	−0.0005 (2)	C8	0.003 (7)
S	0.002 (2)	C9	0.028 (7)
N1	−0.003 (5)	C10	0.024 (6)
N2	−0.006 (5)	C11	0.022 (6)
N3	0.026 (5)	C12	0.023 (7)
C1	0.060 (6)	C13	0.029 (8)
C2	0.111 (7)	C14	0.052 (7)
C3	0.056 (8)	C15	0.034 (7)
C4	0.005 (7)	O2[b]	6.186
C5	−0.029 (6)	O3[b]	6.221
C6	−0.033 (6)	O4[b]	5.866
C7	−0.054 (7)	N4[b]	6.052
	$-0.4557x - 5.952y + 6.889z = -1.719$[a]		
Pt	−0.0000 (2)	N2	−0.004 (5)
S	0.001 (2)	N3	0.013 (5)
N1	0.012 (5)		
	$1.539x - 6.769y + 6.107z = -1.829$[a]		
O2	−0.011 (7)	O4	−0.023 (10)
O3	−0.014 (8)	N4	0.025 (6)

Dihedral Angle		
Plane 1	Plane 2	Angle, deg
Pt, N1, N2	O2, O3, O4	169.5 (4)

[a] See footnote *b*, Table XI, Gill et al., *Inorg. Chem.*, **15**, 1155 (1976). Right side of equation gives distance of plane from origin. [b] Atom at $x, y, z - 1.0$; not used in defining plane.

The crystal structure shows that the mercaptoethanol ligand of $[Pt(terpy)(HET)]^+$ does not interfere with stacking. The conductivity of $[Pt(terpy)(HET)]NO_3$ in water (Figure 3) indicates that it is an ~2:1 electrolyte at concentrations between 10^{-4} and 10^{-2} M, a result consistent with its dimerization constant.

The concentration dependence of the equivalent conductivity of [Pt(terpy)Cl]Cl indicates substantial dimerization in the range 4×10^{-4} to 10^{-2} M. At lower concentrations, the conductivity plot resembles that of a weak electrolyte, suggesting

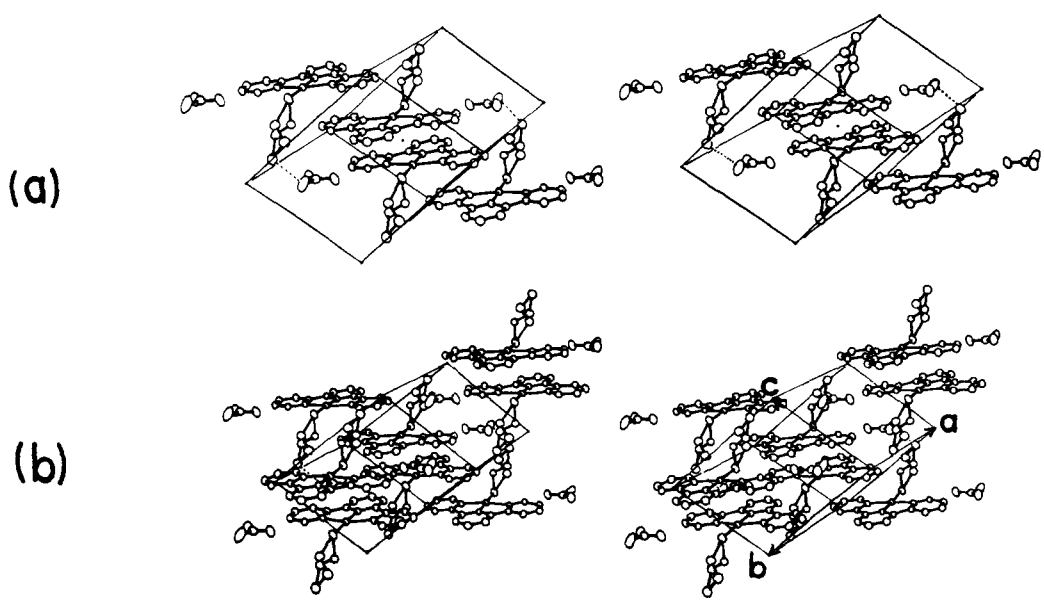

Figure 7. Stereoscopic view of the packing of molecules within and about one unit cell (a) along one axis, and (b) along all three axes. The hydrogen bond is indicated by the dashed lines. The cells shown extend in *a*, *b*, and *c* from $-\frac{1}{2}$ to $\frac{1}{2}$, in fractional coordinates.

dissociation of the labile chloride ion. The pH of a 3.2×10^{-3} M aqueous solution of [Pt(terpy)Cl]Cl is identical with that of water. In nonaqueous solution $[Pt(terpy)(HET)]^+$ is a monomer as, presumably, is $[Pt(terpy)(Cl)]^+$. The electronic spectrum of $[Pt(terpy)Cl]^+$ is very concentration dependent in the absence of added chloride. In 0.1 M sodium chloride Beer's law is obeyed below 15 μM concentration, above which dimerization is indicated. The labile chloride ion in the fourth coordination site and stacking interactions are responsible for this behavior. The large dimerization constant measured spectroscopically for $[Pt(terpy)Cl]^+$ in water, $(4 \pm 2) \times 10^3$ M^{-1}, shows that stacking is quite favorable.

The stacking of square d^8 complexes in their solid lattices is well known.[49] Two types of stacking interactions are seen in $[Pt(terpy)(HET)]NO_3$, as shown in Figure 6. Both stacking patterns show evidence of polar and dipolar interactions.[48] Nitrogen and sulfur atoms, expected to have partial negative charge, situate across from the positive platinum and polarizable, aromatic carbon atoms. The head-to-tail stacking (Figure 6b) of the two cations related by a center of inversion is common to the structures of $[Pd(terpy)Cl]Cl \cdot 2H_2O$,[14] $[Pd(terpy)Cl]_2(PdCl_4)$,[13] and $Pt(bpy)Cl_2$ (red form).[22] The best planes calculated through the platinum atom, sulfur atom, and terpyridine ligand for these two molecules lie 3.43 Å apart. This value compares with that of 3.40 Å for $[Pd(terpy)Cl]Cl \cdot 2H_2O$ and $Pt(bpy)Cl_2$, and 3.52 Å for $[Pd(terpy)Cl]_2(PdCl_4)$. The Pt-Pt distance is 3.5721 (8) Å in $[Pt(terpy)(HET)]NO_3$ and 3.45 Å in $Pt(bpy)Cl_2$. The next closest contact of the platinum atom is with the N1 of the molecule stacked next to it, at a distance of 3.60 Å. This interaction of the metal with the nitrogen on the adjacent molecule is less pronounced than in the [Pd(terpy)Cl]Cl structure where the Pd···N distance is 3.13 Å.

The other stacking arrangement (Figure 6a) shows overlap of two ligand pyridine rings with each other. The distance between the planes through the platinum atom, sulfur atom, and terpyridine ligand for the two molecules is 3.42 Å. Intermolecular platinum contacts are all greater than 3.65 Å. If the platinum nitrogen chelate ring is included, there is good overlap of three coplanar rings in this stacking arrangement. A similarity of $[Pt(terpy)(HET)]^+$ to ethidium is revealed in the stacking patterns of the two molecules (Figure 8). In the crystal structure of ethidium bromide monohydrate,[50] the molecules stack in pairs about centers of symmetry, with a 3.50 Å separation between the planes. The ethyl and phenyl groups of adjacent molecules point in opposite directions, similar to the head-to-tail arrangement seen in $[Pt(terpy)(HET)]^+$. By considering the platinum nitrogen chelate ring as analogous to the center ring of the phenanthridinium ion of ethidium, the overlap patterns of the two compounds are remarkably similar. The structure of Etd $Br \cdot CH_3OH$[51] differs little from that of Etd $Br \cdot H_2O$ in its stacking interactions. The change of the ethyl group of Etd Br to a methyl group alters its stacking pattern considerably.[52] The methyl derivative stacks with planes 3.6 Å apart, with fewer close nitrogen-aromatic carbon contacts, and with the phenyl and methyl groups of the stacked molecules on the same side of the dimer.

Packing. The packing of $[Pt(terpy)(HET)]NO_3$ as sheets in the lattice is shown in Figure 7. Distinct layers containing the platinum atom, sulfur atom, and terpyridine ligand are evident, with the C-C-O moiety of the mercaptoethanol tail projecting between the layers. The cations are laterally displaced from one unit cell to the next, and therefore a columnar stack perpendicular to the terpyridine plane is not generated. This displacement gives rise to two types of close stacking interactions in $[Pt(terpy)(HET)]NO_3$, not seen in the structures of Etd Br[50,51] or proflavine dichloride dihydrate,[53] which pack mainly as dimers. The crystal structure of proflavine hemisulfate[54] reveals less ring system stacking. Two of the four

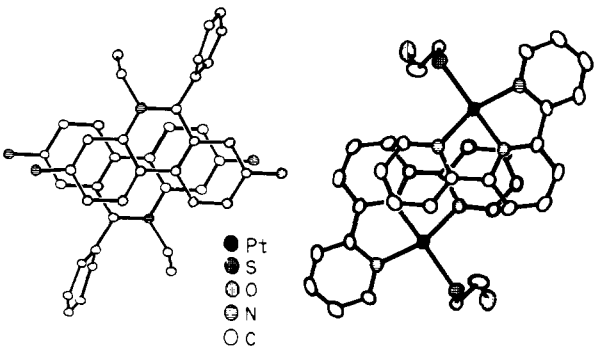

Figure 8. Similarity of the stacking interactions seen in the crystal structures of $[Pt(terpy)(HET)]NO_3$ (right) and Etd Br[50] (left).

molecules in the asymmetric unit are associated, and there is no stacking between adjacent molecules in symmetry-related units. The two proflavine cations that do overlap are separated by about 3.34 Å and are skewed, but have some overlap of all three rings.

Comparison with a Known Intercalator, Etd Br. The properties of $[Pt(terpy)(HET)]NO_3$ and Etd Br are very similar. Both compounds form dimers in aqueous solution and stack in the solid state in a similar manner. All evidence indicates that $[Pt(terpy)(HET)]^+$ intercalates into DNA.[5] Its DNA binding constant is close to that of Etd^+ and is dependent upon salt concentration. The effective diameter of DNA in fibers containing $[Pt(terpy)(HET)]^+$ is virtually the same as in DNA fibers with bound Etd^+.[17] It seems likely, therefore, that the binding modes and overlap with the bases of the two molecules intercalated into DNA are very similar. The hydrogen bonding capability of the mercaptoethanol tail of $[Pt(terpy)(HET)]^+$ may affect the orientation of the molecule with respect to the base pairs which may, therefore, differ from that of Etd^+ in the same site. Etd^+ has two amino groups on the phenanthridinium ring which may enhance intercalative stacking but their importance in hydrogen bonding may be small, since Tsai et al.[55] found only weak interaction of these amino groups with the O-5′ phosphodiester oxygen atom in the structure of Etd^+ intercalated into 5-iodouridylyl(3′-5′)adenosine.

Summary. The present study has provided detailed information about the stacking and hydrogen bond interactions of a metallointercalation reagent, the 2-hydroxyethanethiolato(2,2′,2″-terpyridine)platinum(II) cation, and allowed its comparison to known intercalating drugs such as ethidium bromide. The syntheses of platinum terpyridine complexes with other thiolate ligands have been reported. These metallointercalators enable the study of variations in the fourth ligand on the intercalation process.

Acknowledgment. We are grateful to the National Cancer Institute and the National Science Foundation for financial support, and to the Camille and Henry Dreyfus Foundation for a Teacher-Scholar Grant applied to the purchase of the automated x-ray diffractometer.

Supplementary Material Available: Root-mean-square amplitudes of vibration and observed and calculated structure factor amplitudes (20 pages). Ordering information is given on any current masthead page.

References and Notes

(1) S. J. Lippard, *Prog. Inorg. Chem.*, **18**, vi (1973).
(2) M. Beer and E. N. Moudrianakis, *Proc. Natl. Acad. Sci. U.S.A.*, **48**, 409 (1962).
(3) R. F. Whiting and F. P. Ottensmeyer, *J. Mol. Biol.*, **67**, 173 (1972).
(4) J. Wall, J. Langmore, M. Isaacson, and A. V. Crewe, *Proc. Natl. Acad. Sci. U.S.A.*, **71**, 1 (1974).
(5) (a) K. W. Jennette, S. J. Lippard, G. A. Vassiliades, and W. R. Bauer, *Proc. Natl. Acad. Sci. U.S.A.*, **71**, 3839 (1974); (b) M. Howe-Grant, K. Wu, W. R. Bauer, and S. J. Lippard, *Biochemistry*, in press.
(6) L. S. Lerman, *J. Mol. Biol.*, **3**, 18 (1961).

(7) W. Fuller and M. J. Waring, *Ber. Bunsenges. Phys. Chem.*, **68**, 805 (1964).
(8) D. M. Neville, Jr., and D. R. Davies, *J. Mol. Biol.*, **17**, 57 (1966).
(9) J. Cairns, *Cold Spring Harbor Symp. Quant. Biol.*, **27**, 311 (1962).
(10) (a) D. M. Crothers, *Biopolymers*, **6**, 575 (1968); (b) W. R. Bauer and J. Vinograd, *J. Mol. Biol.*, **47**, 419 (1970).
(11) E. F. Gale, E. Cundliffe, P. E. Reynolds, M. H. Richmond, and M. J. Waring, "The Molecular Basis of Antibiotic Action", Wiley, London, 1972, pp 188–220.
(12) G. T. Morgan and F. H. Burstall, *J. Chem. Soc.*, 1498 (1934).
(13) G. M. Intille, Ph.D. Dissertation, Syracuse University, Syracuse, N.Y., 1967.
(14) G. M. Intille, C. E. Pfluger, and W. A. Baker, Jr., *J. Cryst. Mol. Struct.*, **3**, 47 (1973).
(15) F. Basolo, H. B. Gray, and R. G. Pearson, *J. Am. Chem. Soc.*, **82**, 4200 (1960).
(16) C. H. Langford and H. B. Gray, "Ligand Substitution Processes", W.A. Benjamin, New York, N.Y., 1965, pp 18–54.
(17) P. J. Bond, R. Langridge, K. W. Jennette, and S. J. Lippard, *Proc. Natl. Acad. Sci. U.S.A.*, **72**, 4825 (1975).
(18) G. Schwarz, S. Klose, and W. Balthasar, *Eur. J. Biochem.*, **12**, 454 (1970).
(19) G. P. Kreishman, S. I. Chan, and W. Bauer, *J. Mol. Biol.*, **61**, 45 (1971).
(20) (a) G. Thomas and B. Roques, *FEBS Lett.*, **26**, 169 (1972); (b) D. M. Crothers, private communication.
(21) N. S. Angerman, T. A. Victor, C. L. Bell, and S. S. Danyluk, *Biochemistry*, **11**, 2402 (1972).
(22) (a) R. S. Osborn and D. Rogers, *J. Chem. Soc., Dalton Trans.*, 1002 (1974); (b) D. Rogers, private communication.
(23) (a) W. Müller and D. M. Crothers, *Eur. J. Biochem.*, **54**, 267 (1975); (b) W. Müller, H. Bünemann, and N. Dattagupta, *ibid.*, **54**, 279 (1975); (c) E. J. Gabbay, R. E. Scofield, and C. S. Baxter, *J. Am. Chem. Soc.*, **95**, 7850 (1973), and references cited therein.
(24) (a) J.-B. LePecq, M. LeBret, J. Barbet, and B. Roques, *Proc. Natl. Acad. Sci. U.S.A.*, **72**, 2915 (1975); (b) E. S. Canellakis, Y. H. Shaw, W. E. Hanmers, and R. A. Schwartz, *Biochim. Biophys. Acta*, **418**, 277 (1976).
(25) R. D. Feltham and R. G. Hayter, *J. Chem. Soc.*, 4587 (1964).
(26) W. E. Parham, H. Wynberg, and F. L. Ramp, *J. Am. Chem. Soc.*, **75**, 2065 (1953).
(27) Programs for IBM 360-91 computer used in this work: UMAT, the local version of the Brookhaven diffractometer setting and cell constant and orientation refinement program; ORABS, the local version of the absorption correction program by D. J. Wehe, W. R. Busing, and H. A. Levy, adapted to FACS-I geometry; XDATA, the Brookhaven Wilson plot and scaling program; FOURIER, the Zalkin Fourier program; CUGLS, the local version of the Busing–Martin–Levy structure factor calculation and least-squares refinement program (ORFLS) modified by Ibers and Doedens for rigid-body refinement; ORFFE, the Busing–Martin–Levy molecular geometry and error function program; TRACER II, the Lawton lattice transformation–cell reduction program; and ORTEP II, the Johnson thermal ellipsoid plotting program; in addition to various local data processing programs.
(28) B. G. Segal and S. J. Lippard, *Inorg. Chem.*, **13**, 822 (1974).
(29) J. T. Gill and S. J. Lippard, *Inorg. Chem.*, **14**, 751 (1975).
(30) "International Tables for X-Ray Crystallography", Vol. III, Kynoch Press, Birmingham, England, 1962, pp 162–163.
(31) A. J. C. Wilson, *Nature (London)*, **150**, 151 (1942).
(32) $R_1 = \sum||F_o| - |F_c||/\sum|F_o|$ and $R_2 = [\sum w(|F_o| - |F_c|)^2/\sum w|F_o|^2]^{1/2}$, where $w = 4F_o^2/\sigma^2(F_o^2)$. The function $\sum w(|F_o| - |F_c|)^2$ was minimized.
(33) Atom scattering factors (and anomalous dispersion corrections for Pt and S atoms): "International Tables for X-Ray Crystallography", Vol. IV, Kynoch Press, Birmingham, England, 1974, Tables 2.2A (and 2.3.1).
(34) D. W. J. Cruickshank in "Computing Methods of Crystallography", J. S. Rollett, Ed., Pergamon Press, New York, N.Y., 1965, pp 112–115.
(35) (a) S. Castellano, H. Gunther, and S. Ebersole, *J. Phys. Chem.*, **69**, 4166 (1965); (b) F. E. Lytle, L. M. Petrosky, and L. R. Carlson, *Anal. Chim. Acta*, **57**, 239 (1971); (c) E. Bielli, P. M. Gidney, R. D. Gillard, and B. T. Heaton, *J. Chem. Soc., Dalton Trans.*, 2133 (1974).
(36) D. A. Ucko and S. J. Lippard, unpublished results.
(37) L. Pauling, "The Nature of the Chemical Bond", 3d ed, Cornell University Press, Ithaca, N.Y., 1960, p 260.
(38) (a) H. Booth and A. H. Bostock, *Chem. Commun.*, 637 (1967); (b) R. A. Bauman, *J. Org. Chem.*, **32**, 4129 (1967); (c) *Tetrahedron Lett.*, 419 (1971); (d) R. Gallo, A. Liden, C. Roussel, J. Sandström, and J. Metzger, *Tetrahedron Lett.*, 1985 (1975).
(39) L. E. Erickson, J. E. Sarneski, and C. N. Reilley, *Inorg. Chem.*, **14**, 3007 (1975).
(40) W. J. Geary, *Coord. Chem. Rev.*, **7**, 81 (1971).
(41) R. G. Hayter and F. S. Humiec, *Inorg. Chem.*, **2**, 306 (1963).
(42) See paragraph at end of paper regarding supplementary material.
(43) E. Goldschmied and N. C. Stephenson, *Acta Crystallogr., Sect. B*, **26**, 1867 (1970).
(44) F. W. B. Einstein and B. R. Penfold, *Acta Crystallogr.*, **20**, 924 (1966).
(45) M. R. Caira and L. R. Nassimbeni, *Acta Crystallogr., Sect. B*, **31**, 581 (1975).
(46) R. Melanson, J. Hubert, and F. D. Rochon, *Can. J. Chem.*, **53**, 1139 (1975).
(47) L. L. Merritt, Jr., and E. D. Schroeder, *Acta Crystallogr.*, **9**, 801 (1956).
(48) (a) B. Pullman and A. Pullman, *Prog. Nucleic Acid Res. Mol. Biol.*, **9**, 327 (1969); (b) C. E. Bugg, J. M. Thomas, M. Sundaralingam, and S. T. Rao, *Biopolymers*, **10**, 175 (1971).
(49) J. S. Miller and A. J. Epstein, *Prog. Inorg. Chem.*, **20**, 1 (1976).
(50) E. Subramanian, J. Trotter, and C. E. Bugg, *J. Cryst. Mol. Struct.*, **1**, 3 (1971).
(51) M. Hospital and B. Busetta, *C. R. Acad. Sci., Ser. C*, **268**, 1232 (1969).
(52) C. Courseille, B. Busetta, and M. Hospital, *C. R. Acad. Sci., Ser. C*, **275**, 95 (1972).
(53) S. K. Obendorf, H. L. Carrell, and J. P. Glusker, *Acta Crystallogr., Sect. B*, **30**, 1408 (1974).
(54) S. Neidle and T. A. Jones, *Nature (London)*, **253**, 284 (1975).
(55) C.-C. Tsai, S. C. Jain, and H. M. Sobell, *Proc. Natl. Acad. Sci. U.S.A.*, **72**, 628 (1975).

Applications of Artificial Intelligence for Chemical Inference. 22. Automatic Rule Formation in Mass Spectrometry by Means of the Meta-DENDRAL Program[1a]

B. G. Buchanan,* D. H. Smith, W. C. White, R. J. Gritter,[1b] E. A. Feigenbaum, J. Lederberg, and Carl Djerassi

Contribution from the Departments of Computer Science, Chemistry, and Genetics, Stanford University, Stanford, California 94305. *Received January 27, 1976*

Abstract: The DENDRAL computer program uses established rules of molecular fragmentation to help chemists solve complex structural problems from mass spectral data. This paper describes a computer program called Meta-DENDRAL, that can aid in the discovery of such rules from empirical data on known compounds. The program uses heuristic methods to search for common structural environments around those bonds that are found to fragment and abstracts plausible fragmentation rules. The program has been tested on the well-characterized, low-resolution mass spectra of aliphatic amines and the high-resolution mass spectra of estrogenic steroids. The program has also discovered new fragmentation rules for mono-, di-, and triketoandrostanes.

The DENDRAL computer program is designed to aid chemists with complex structure elucidation problems. One main part uses established molecular fragmentation rules to help chemists interpret mass spectra;[2] another main part generates lists of isomers that satisfy constraints derived from a variety of spectroscopic techniques.[3] Because the mass spectrometry rules used by the DENDRAL program have been culled from the literature, the program's growth depends upon manual examination of collections of spectra. But investigating the spectral data of new compound classes to determine frag-